Continuous spectra of atomic hydrogen in a strong magnetic field

L. B. Zhao,[1,2] O. Zatsarinny,[2] and K. Bartschat[2]
[1]*School of Physics and Electronic Engineering, Harbin Normal University, Harbin 150025, China*
[2]*Department of Physics and Astronomy, Drake University, Des Moines, Iowa 50311, USA*
(Received 6 August 2016; published 29 September 2016)

We describe a theoretical method, developed in the coupled-channel formalism, to study photoionization of H atoms in a strong magnetic field of a size that is typical for magnetic white dwarfs. The coupled Schrödinger equations are solved numerically using the renormalized Numerov method proposed by Johnson [B. R. Johnson, J. Chem. Phys. **67**, 4086 (1977); **69**, 4678 (1978)]. The distinct advantage of this method is the fact that no overflow problems are encountered in the classically forbidden region, and hence the method exhibits excellent numerical stability. Photoionization cross sections are presented for magnetized H atoms in the ground and $2p$ excited states. The calculated results are compared with those obtained by other theories. The present method is particularly useful for explaining the complex features of continuous spectra in a strong magnetic field and hence provides an efficient tool for modeling photoionization spectra observed in the atmosphere of magnetic white dwarfs.

DOI: 10.1103/PhysRevA.94.033422

I. INTRODUCTION

Investigations of spectra of magnetized atoms are of special importance to understand the evolution of normal stars to magnetic white dwarf stars (magnetic fields of 10^2–10^5 T) and neutron stars (10^7–10^9 T). The initial magnetic fields in stars are believed to increase with their evolution [1]. The components of the atmospheres of white dwarf and neutron stars, as well as the size of their magnetic field strengths, may be determined by comparing computed and observed spectrum lines. During the past few decades, many astronomically observed spectra of magnetized atoms have been reported, and a great deal of effort has been devoted to developing theories and numerical algorithms for describing the properties of magnetized atoms. Although steady progress has been made, theories and computations are still far from meeting the requirements for simulating the astronomically observed spectra [2,3]. Today, it is regarded a considerable success to be able to accurately model the discrete spectra of magnetized H atoms [4]. High-accuracy spectra for any transition between bound states of H atoms in an arbitrary magnetic field, obtained with several theoretical methods, have been reported in the literature [4–7].

Going beyond atomic hydrogen, even the simulation of the discrete spectra of multielectron atoms in a strong magnetized field is highly challenging due to the theoretical difficulties associated with an efficient and accurate treatment of electron correlations in a strong magnetic field. Most calculations of atomic structures of magnetized multielectron atoms published to date have been performed within the framework of Hartree-Fock theory (see, for example, Refs. [8–11] and references therein). Electron correlations in a magnetic field have been effectively taken into account only for the light helium atom [12,13].

Compared to discrete spectra of atoms in a magnetic field of white-dwarf strength, their continuous spectra are only sparsely reported in the literature. A few theoretical and computational attempts have been implemented. Alijah *et al.* [14] constructed a coupled-channel theory to describe photoionization of strongly magnetized H atoms. They expanded the total wave function in terms of Landau states. The resulting coupled Schrödinger equations were solved with a stable numerical integration procedure based on the logarithmic derivative method, proposed by Johnson [15], with some modifications. The photoionization spectrum was presented for the initial ground state in a magnetic field of 2000 T, and a Rydberg series of resonance states was identified.

By combining a complex-rotation technique with a Sturmian-type basis expansion, Delande *et al.* [16] developed a theoretical method to yield continuous spectra of strongly magnetized H atoms, and they applied it to calculations of photoionization from the ground state in a magnetic field of 23 500 T. Today, this spectrum has become the benchmark for testing the reliability of later theories. Soon afterwards, Wang and Greene [17] presented their R-matrix calculations of ground-state H atoms in a strong magnetic field, based on a method developed within the framework of multichannel quantum-defect theory (MQDT). However, they did not reproduce the photoionization spectrum of Alijah *et al.* [14] at 2000 T, but rather found a pronounced difference.

Based on the complex-rotation method combined with a mixed Slater-Landau basis expansion, Zhao and Stancil [18] also developed a computational scheme to describe the photoionization of atomic hydrogen in strong magnetic fields. Since the basis expansion of this scheme explicitly incorporates the physics of the strong-field regime, it can cover a wide field region more efficiently than previously reported methods. The scheme was successfully applied to photoionization calculations for 12 initial states with magnetic field strengths from 2350 T to 235 000 T [19]. Furthermore, Meinhardt and co-workers [20] presented their coupled-channel results for the continuous spectra of magnetized H atoms. They found them to be in excellent agreement with those from both the complex-rotation method [16] and the R-matrix method [17], but once again not with those of Alijah *et al.* [14].

More recently, Mota-Furtado and O'Mahony [21] proposed an R-matrix propagation technique with adiabatic bases to calculate the photoionization spectra of atoms in magnetic fields. In their scheme, the configuration space is divided

into many subregions. In each subregion, the R matrix is propagated, and then continuity of the wave functions and their derivatives is enforced at the boundaries between all subregions. While this propagation technique was successful, it needs to be generalized to deal with higher magnetic field strengths that significantly distort the field-free wave functions of the atoms in the inner region [21]. Since any complex-rotation method fails to represent the overall perspective of Rydberg structures due to the limitation of a finite basis, our previous method described in Ref. [18] cannot be utilized to elucidate the remaining differences between the photoionization spectra obtained by a variety of theoretical methods. It is hence necessary to develop a different method to effectively describe photoionization near the ionization threshold. The work reported in this paper is devoted to this goal.

This manuscript is organized as follows. Section II describes the coupled-channel formalism for photoionization of atomic hydrogen in a strong magnetic field typical of magnetic white dwarf stars. The numerical method to solve the coupled Schrödinger equations for obtaining the wave functions of the final continuum states is outlined, and solutions for the initial bound states in a magnetic field are recapitulated. In Sec. III, we apply our method to study photoionization of magnetized H atoms. Photoionization spectra for the ground state and some excited states are presented and comparison is made with predictions from other theories. Section IV summarizes our principal results and contains some concluding remarks. Unless specified otherwise, atomic units (a.u.) are used throughout this paper.

II. THEORETICAL METHOD

This section is devoted to the description of the coupled-channel formalism for magnetized hydrogen atoms, the outline of the numerical method to solve the coupled Schrödinger equations for the continuum states, and the sketch of the solutions for the bound states in a magnetic field.

A. Coupled-channel formalism

In this section, we formulate the standing-wave solutions as well as the incoming- and outgoing-wave solutions of the coupled Schrödinger equations. Within the framework of nonrelativistic theory, the Hamiltonian of H atoms in a uniform magnetic field B along the z axis is given by

$$\widehat{H} = -\frac{1}{2}\nabla^2 - \frac{1}{\sqrt{\rho^2+z^2}} + \frac{\gamma}{2}(\hat{\ell}_z + 2\hat{s}_z) + \frac{1}{8}\gamma^2\rho^2. \quad (1)$$

Here $\gamma = B/B_0$ is the magnetic field strength in atomic units, i.e., in multiples of $B_0 \simeq 2.35 \times 10^5$ T. Using cylindrical coordinates (ρ,z), $\hat{\ell}_z$ and $\hat{s}_z$ are the operators for the z components of the orbital and spin angular momenta, respectively. The third term (linear in γ) is the paramagnetic potential, while the fourth term (quadratic in γ) is the diamagnetic potential. Depending on the relative magnitudes of the Coulomb and diamagnetic potentials, the symmetry of the system changes. The system more resembles spherical symmetry if the Coulomb potential dominates the diamagnetic potential, whereas it is closer to cylindrical symmetry in the opposite case. For strong magnetic fields, therefore, the system is most conveniently described in cylindrical coordinates.

We expand the total wave function in terms of Landau states as

$$\Psi(\rho,\phi,z) = \sum_{n'} \mathcal{R}_{n'}(\rho,\phi)\mathcal{F}_{n'}(z) = \sum_{n'} \mathscr{R}_{n'}(\rho)\frac{e^{im\phi}}{\sqrt{2\pi}}\mathcal{F}_{n'}(z), \quad (2)$$

where $\mathcal{R}_n(\rho,\phi)$ is the normalized wave function for the Landau state with $n \geqslant 0$, given in Ref. [22] as

$$\mathcal{R}_n(\rho,\phi) = \frac{\gamma^{(|m|+1)/2}}{m!}\sqrt{\frac{(|m|+n)!}{2^{|m|}n!}}e^{-\rho^2\gamma/4}\rho^{|m|} \times {}_1F_1(-n,|m|+1,\rho^2\gamma/2)\frac{e^{im\phi}}{\sqrt{2\pi}}, \quad (3)$$

with ${}_1F_1$ denoting the confluent hypergeometric function and m the magnetic quantum number. Substituting Eq. (2) into the Schrödinger equation with the Hamiltonian (1) and projecting onto the basis $\mathcal{R}_n$, we obtain the following set of coupled differential equations:

$$\left[-\frac{1}{2}\frac{d^2}{dz^2} - \varepsilon_n\right]\mathcal{F}_n + \sum_{n'} V_{nn'}\mathcal{F}_{n'} = 0, \quad (4)$$

where $\varepsilon_n = E - E_n$. Here E denotes the energy of the free electron and $E_n = \gamma[n + (|m| + m + 1)/2]$ the energy of the Landau state. For simplicity of notation, we omit the energy E in the argument of $\mathcal{F}_n$, as well any function below that is constructed from these continuum solutions.

The matrix element $V_{nn'}(z)$ is given in Ref. [23] as

$$V_{nn'}(z) = -\int_0^\infty \mathscr{R}_{n'}(\rho)\frac{1}{\sqrt{\rho^2+z^2}}\mathscr{R}_n(\rho)\rho\,d\rho = -\frac{2}{\sqrt{\pi}}\sum_{j=0}^{\min(n',n)}\frac{[n'!n!(n'+|m|)!(n+|m|)!]^{1/2}}{(n'-j)!(n-j)!(|m|+j)!j!} \times \mathcal{I}(n'+n-2j,2j+|m|;z), \quad (5)$$

with

$$\mathcal{I}(\alpha,\beta;z) = \sqrt{\frac{\gamma}{2}}\int_0^{\pi/2}(\sin x)^{2\beta}(\cos x)^{2\alpha}\exp\left[-\frac{\gamma z^2\cos^2 x}{2\sin^2 x}\right]dx. \quad (6)$$

As seen from Eq. (4), the presence of the Coulomb potential couples the Landau channels. Since each linearly independent solution should be a linear combination of the channel wave functions, it is essential to introduce an additional subscript n to identify these solutions. Thus we adopt the indices n' and n in $\mathcal{F}_{n'n}$ to identify the channel and the solution, respectively. Equation (2) is then rewritten as

$$\Psi_n(\rho,\phi,z) = \sum_{n'} \mathcal{R}_{n'}(\rho,\phi)\mathcal{F}_{n'n}(z). \quad (7)$$

It was shown in Refs. [14,21] that the free electron feels a Coulomb potential in the asymptotic region at large z. Therefore, $\mathcal{F}_{n'n}(z)$ should asymptotically have the form

$$\mathcal{F}_{n'n} = s_n\delta_{n'n} + c_n\mathcal{K}_{n'n}, \quad (8)$$

where s_n and c_n, respectively, are regular and irregular Coulomb functions as defined by Seaton [24], and $\mathcal{K}_{n'n}$ is the matrix element of the reactance matrix $\mathcal{K}$.

In compact matrix notation, Eq. (8) reads

$$\mathcal{F} = s + c\,\mathcal{K}. \tag{9}$$

If all channels are open, $\mathcal{F}$ represents a matrix of the physical standing-wave solutions of the coupled Schrödinger equations. However, $\mathcal{F}$ contains exponentially growing terms in any closed channel, and these correspond to unphysical solutions.

In order to formulate physically meaningful solutions, therefore, the matrices $\mathcal{F}$ and $\mathcal{K}$ are each partitioned into open-open, open-closed, closed-open, and closed-closed submatrices, as suggested by Seaton [24]. Generically denoting these matrices by $\mathcal{A}$ for simplification, we have

$$\mathcal{A} = \begin{pmatrix} \mathcal{A}_{oo} & \mathcal{A}_{oc} \\ \mathcal{A}_{co} & \mathcal{A}_{cc} \end{pmatrix}. \tag{10}$$

Using these submatrices, physical standing-wave solutions F are constructed by imposing physical boundary conditions,

$$\begin{pmatrix} F_{oo} \\ F_{co} \end{pmatrix} = \begin{pmatrix} \mathcal{F}_{oo} & \mathcal{F}_{oc} \\ \mathcal{F}_{co} & \mathcal{F}_{cc} \end{pmatrix} \begin{pmatrix} L_{oo} \\ L_{co} \end{pmatrix}, \tag{11}$$

where the subscripts o and c denote the *open* and *closed* channels, L_{oo} is the identity matrix, and

$$L_{co} = -[\tan(\pi\nu) + \mathcal{K}_{cc}]^{-1}\mathcal{K}_{co}, \tag{12}$$

with ν denoting the effective quantum number. The physical reactance matrix K_{oo} (open channels only) is given by

$$K_{oo} = \mathcal{K}_{oo} + \mathcal{K}_{oc}L_{co}. \tag{13}$$

Finally, the incoming- and outgoing-wave solutions of the coupled Schrödinger equations are expressed as

$$F^{\pm} = \mp i\,F(I \mp K)^{-1}. \tag{14}$$

Note that the parity of $F(z)$ under the transformation $z \to -z$ (denoted by $\pi_z = \pm 1$ for even or odd parity) should be conserved. Hence, π_z and the other good quantum number m (the projection of the orbital angular momentum on the z axis) together are adopted to identify the hydrogen atomic states m^{π_z} in a magnetic field.

B. Numerical integration of the coupled equations

In matrix notation, the coupled-channel Schrödinger equations (4) are written as

$$\left[I\frac{d^2}{dz^2} + Q(z)\right]\mathcal{F}(z) = 0, \tag{15}$$

where I denotes the identity matrix, and the matrix elements of Q are given by

$$Q_{nn'}(z) = 2\,\varepsilon_n\delta_{nn'} - 2\,V_{nn'}(z). \tag{16}$$

In the present work, we adopt Johnson's algorithm [25] to numerically integrate the coupled differential equations (15). This algorithm propagates the ratio of the wave function at a given mesh point and the adjacent point, rather than the wave function itself. Since it efficiently avoids potential overflow problems of the wave function in the classically forbidden region, it is apparently superior to numerical methods that propagate the wave function itself. In matrix notation, the ratio is defined by

$$R_n = (I - T_{n+1})\mathcal{F}_{n+1}\mathcal{F}_n^{-1}(I - T_n)^{-1}, \tag{17}$$

where $T_n = -\frac{h^2}{12}Q_n$, with h being the step size of the integration. Setting

$$U_n = (I - T_n)^{-1}(2I + 10\,T_n), \tag{18}$$

the ratio matrix is propagated from the origin in terms of the two-term recurrence relation

$$R_n = U_n - R_{n-1}^{-1}. \tag{19}$$

The wave function at the origin is zero for states of odd parity, while its derivative is zero at this point for states with even parity. These properties of the wave functions and their derivatives are exploited to obtain the ratio R_0 at the origin. It is determined to be

$$R_0 = \begin{cases} \infty & \text{for odd parity,} \\ (I + 5T_0)(I - T_0)^{-1} & \text{for even parity.} \end{cases} \tag{20}$$

In practical calculations, R_0 for the odd-parity states is taken as a large number, e.g., 10^{30}. Our numerical integration begins from the origin and stops in the asymptotic region, where we match the numerical ratio matrix R to the ratio matrix calculated with the asymptotic forms given in Eq. (9) to extract the reaction matrix $\mathcal{K}$. We then apply the procedure described in the preceding section to calculate the standing-wave solutions and then construct incoming- or outgoing-wave solutions of the coupled Schrödinger equations with physical boundary conditions. Finally, the wave functions obtained in this way are utilized to calculate dipole matrix elements, photoionization cross sections, and oscillator strengths.

C. Solutions for bound states in a magnetic field

In magnetic fields of white-dwarf strength, it is inevitable to consider the influence of such strong fields on the initial atomic states in photoionization. In order to do this, we apply our finite-basis-set method with B splines developed previously [26] to calculate the low-lying atomic states in a strong magnetic field. Using a representation in spherical coordinates, the total wave functions are expanded in terms of a B-spline basis in the radial direction and spherical harmonics for the angular part. Due to the nonorthogonality inherent in a B-spline basis, the solution of the resulting matrix equations is a generalized eigenvalue problem involving the decomposition of the overlap matrices. Once the decomposition has been done, standard routines for matrix diagonalization are used to generate the eigenvalues and eigenvectors numerically. Finally, the eigenvectors obtained in this way are mapped to the cylindrical coordinate system and subsequently applied to the calculations of the dipole matrix elements.

D. Differential oscillator strength and cross sections for photoionization

The numerically obtained wave functions for the initial bound and final continuum states, denoted by Ψ_i and Ψ_n^-, respectively, are then utilized to calculate differential (with

respect to energy and state) oscillator strengths and cross sections for photoionization. The differential oscillator strength for magnetized H atoms in the photoionization process from an initial state with energy E_i to a final state with energy E is given by

$$\frac{df_{n,i}}{dE} = 2(E - E_i)|\langle\Psi_n^-|D|\Psi_i\rangle|^2, \tag{21}$$

where D is the dipole operator and Ψ_n^- is defined by

$$\Psi_n^-(\rho,\phi,z) = \sum_{n'} \mathcal{R}_{n'}(\rho,\phi)F_{n'n}^-(z). \tag{22}$$

The total differential (with respect to energy) oscillator strength is an astronomically observable quantity. It is obtained by summing the differential oscillator strengths for photoionization into the individual state according to

$$\frac{df_i}{dE} = \sum_n \frac{df_{n,i}}{dE}. \tag{23}$$

The photoionization cross section is related to the total differential oscillator strength by

$$\sigma_i(E) = 2\pi^2\alpha\frac{df_i}{dE}, \tag{24}$$

where $\alpha \approx 1/137$ is the fine-structure constant.

Looking at the literature in this field, we note that different authors preferred to present their results either as cross sections or as oscillator strengths, in both cases usually with the independent variable chosen as the ejected electron energy E. The latter is related to the photon energy ω through $E = \omega + E_i$. To simplify the visual comparison with previous works (numerical data are not available, and the spectra are too complex for digitizing the graphs), we generally adapt our presentation below and follow previous authors.

III. RESULTS AND DISCUSSION

The coupled-channel formalism described above was applied to study the photoionization of H atoms in strong magnetic fields. First of all, we tested our method by comparing the results with the accepted benchmark spectrum for photoionization from the ground state. We assumed that H atoms in the ground state were placed in a uniform magnetic field of strength $B = 0.1$ a.u. (23 500 T). They were then irradiated by a beam of linearly polarized light with the polarization direction parallel to the magnetic field and ionized into the final continuum state with $m^{\pi_z} = 0^-$.

We checked the convergence of the predicted photoionization cross sections by varying the number of coupled channels as well as $z_{\max}$, where the ratio matrix R is matched to the asymptotic form to extract the reactance matrices. We found that seven coupled channels and $z_{\max} = 30$ a.u. were sufficient to obtain the converged spectrum shown in Fig. 1.

While we do not have access to their actual data, comparison with the figures shows excellent visual agreement between our results and those from other theories [16–18,21]. On the other hand, the complex-rotation calculations reported in Refs. [16,18] fail to represent the overall Rydberg structures near the ionization thresholds. The detailed information about the complex structures associated with high-lying Rydberg states is lost in the complex-rotation calculations. This is not surprising in light of the fact that the rotated continua are represented by a set of discrete eigenvalues in the complex-rotation method, and the imaginary parts of the discrete eigenvalues in the close vicinity of a Landau threshold are very small. It is simply impossible to describe an infinite Rydberg series with a finite basis.

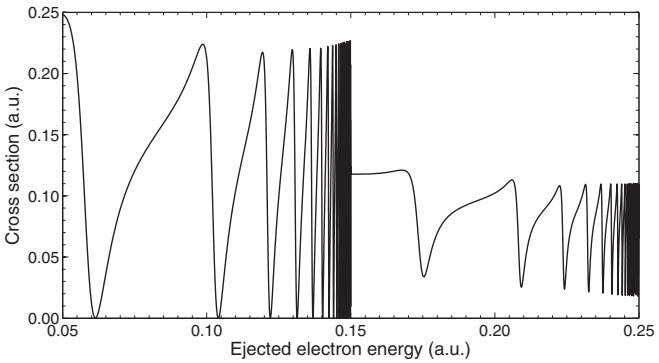

FIG. 1. Photoionization spectrum for magnetized hydrogen atoms in a magnetic field of $B = 0.1$ a.u. (23 500 T). It is assumed that the atoms in the ground state are irradiated by a beam of linearly polarized light and, therefore, ionized to the final state $m^{\pi_z} = 0^-$. The energy region covers a range from the first up to the third Landau threshold. The convergence of the Rydberg series towards the second and third Landau thresholds with energies of 0.15 and 0.25 a.u., respectively, is clearly visible.

To further test our method, it is essential to compare our results with other photoionization spectra. Figure 2 illustrates our spectra at $B = 0.05$ a.u. (11 750 T) for photoionization from the ground state to the final continuum states $m^{\pi_z} = 1^+$ and 0^-. The two spectra display regular patterns of broad resonances embedded in narrow dense resonances associated with high-lying Rydberg states. Such a phenomenon was also noticed and discussed by Wang and Greene [17]. The resonances associated with different Rydberg series interfere with each other and hence generate very complex patterns in the spectra. The two spectra due to photoionization from the ground state into the final continuum states with $m^{\pi_z} = 1^+$ and 0^- are found to be in excellent agreement with those presented in Ref. [17].

We now move on to the photoionization spectrum of H atoms in a magnetic field with strength $B = 0.0085$ a.u. (2000 T). Here the spectrum of interest concerns photoionization of magnetized ground-state hydrogen atoms irradiated by a beam of circularly polarized light. The final continuum state is thus $m^{\pi_z} = 1^+$. The ejected-electron energy range shown in the insert of Fig. 3 covers the narrow region from 0.0280 to 0.02977 a.u., i.e., between the second and third Landau thresholds.

Looking at the respective papers [14,17,20], one will notice a pronounced discrepancy between the spectra calculated by three groups. Our calculations contain two open and 12 closed channels. Choosing $z_{\max} = 80$ a.u. yields convergence of the predicted photoionization cross sections. Alijah *et al.* [14], on the other hand, also included two open but only eight closed channels, and they set $z_{\max} = 50$ a.u. While the authors claimed to have obtained a convergent spectrum, we could

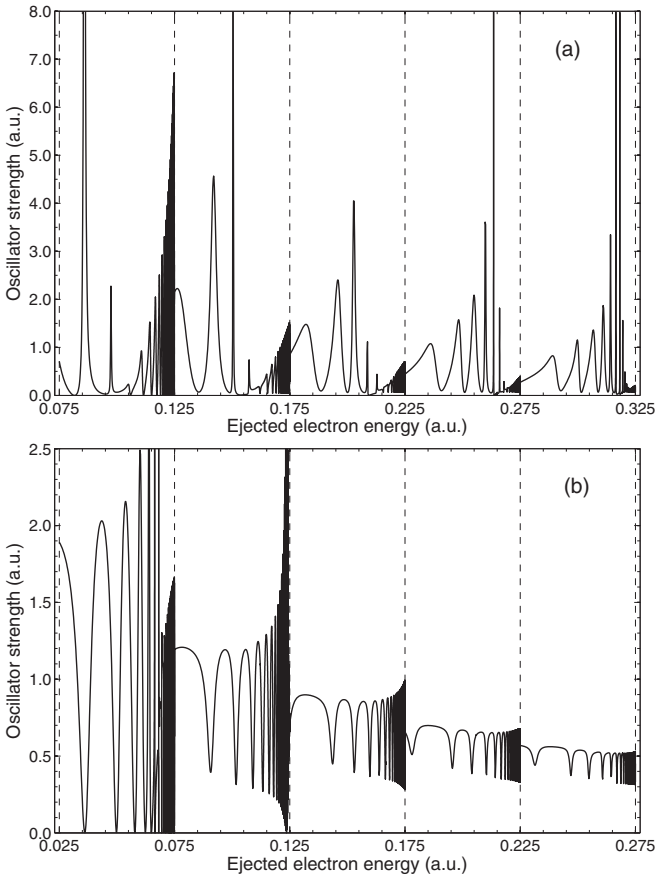

FIG. 2. Photoionization spectra of magnetized hydrogen atoms from the ground state to the final states $m^{\pi_z} = 1^+$ (a) and $m^{\pi_z} = 0^-$ (b) at $B = 0.05$ a.u. (11 750 T). The ejected-electron energies cover the range from the first to the sixth Landau threshold. The dashed vertical lines indicate all the Landau thresholds in this regime.

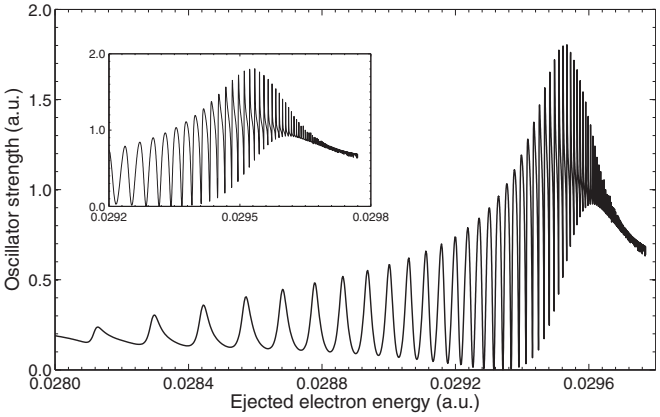

FIG. 3. Photoionization spectrum for magnetized hydrogen atoms from the ground state into the final continuum state $m^{\pi_z} = 1^+$ at $B = 0.0085$ a.u. (2000 T). The insert corresponds to the energy regime used by Wang and Greene [17] in the bottom part of their Fig. 6 to compare with the results of Alijah *et al.* [14]. For consistency, we use the same energy scale in all our figures, and hence we subtracted the electron paramagnetic spin energy of 0.004 255 3 a.u. from the scale used by Alijah *et al.* [14].

not reproduce the results of Alijah *et al.* [14] with the same parameters.

The R-matrix method based on MQDT developed by Wang and Greene [17] did not reproduce the spectrum of Alijah *et al.* [14] either, and neither did the direct numerical integration method of Meinhardt and co-workers [20]. The latter authors suspected that nondecaying closed-channel solutions in Ref. [14] caused inaccuracies in their calculations of the transition matrix elements. Unfortunately, Meinhardt *et al.* [20] only discussed the spectrum, but no illustration was provided.

While we obtain at least qualitative agreement with Wang and Greene [17] (see their Fig. 6), we do not agree with them in all details of their predictions. The latter authors carefully tested the sensitivity of their calculated spectrum to variations of the numerical parameters, for example, by increasing the cylindrical R-matrix box size z_0 and by changing the number of coupled-channel numbers. They found that the individual resonance positions, widths, and shapes change substantially with variations in those two parameters. Their predicted spectrum reaches convergence with $z_0 = 80$ a.u. and a total of 12 channels, which are essentially our parameters. Looking at their Fig. 6 in detail, it appears as if Wang and Greene [17] did not resolve the detailed resonance structure in this very narrow energy regime. They found the oscillator strength to oscillate around 0.7, which is in reasonable agreement with our predictions if the latter were convoluted with a Gaussian of realistic width.

Having found some quantitative disagreement with the results of Wang and Greene [17], it seemed important to investigate some more cases, particularly at lower field strengths. Figure 4 exhibits our results for $B = 0.01$ a.u. (2350 T) for the initial $1s_0$ state and the final continuum states $m^{\pi_z} = 1^+$ and $m^{\pi_z} = 0^-$. Since the energy-resolved spectra are very complex, we follow Wang and Greene [17] and also present our results after convolution with Gaussians of width 0.0025 and 0.0009 a.u., respectively. The figure corresponds to about half the energy range presented in Figs. 2 and 4 of Wang and Greene [17]. Looking at those figures and comparing with our results, one will notice significant differences in the details. While the convoluted results from their and our calculations are still in qualitative agreement, they do not agree as well with each other as even the unconvoluted results did at the higher field strengths. Without knowing the numerical details of their method, we refrain from speculating about potential reasons for the remaining disagreement. We note, however, that Wang and Greene [17] themselves expressed some caution regarding the reliability of their results at relatively low field strengths.

Having gained sufficient confidence in our approach, we now present additional results. The photoionization cross sections from the $2p_0$ excited state to the final state with $m^{\pi_z} = 1^-$ at $B = 0.1$ a.u. (23 500 T) are shown in Fig. 5 as a function of the ejected-electron energy. The figure exhibits rich resonance structures converging to the second and third Landau thresholds. Such resonance structures have been observed in photoionization from the ground state to the final continuum $m^{\pi_z} = 0^-$, as shown in Fig. 1.

These resonances are associated with quasibound Coulombic states embedded in the Landau continua. From the spectrum, one can obtain insight into interactions between the

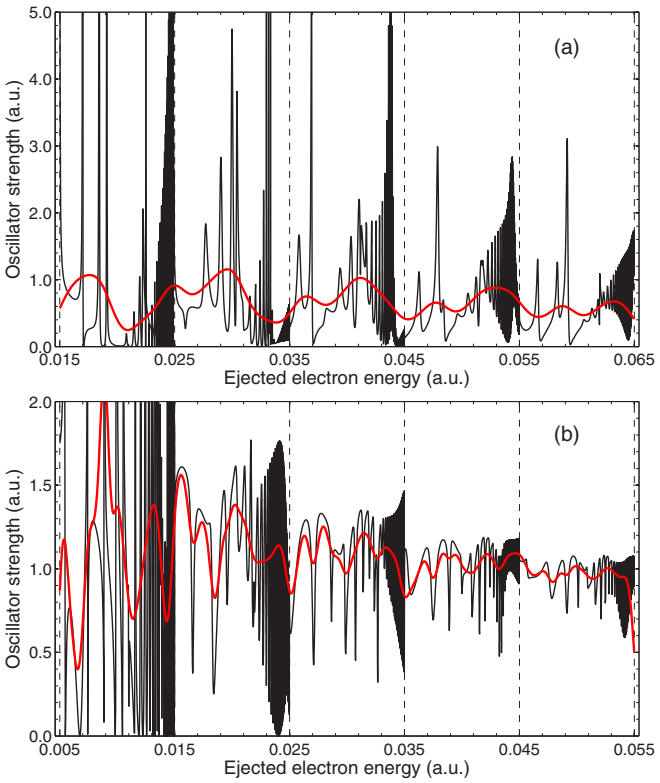

FIG. 4. Photoionization spectrum for magnetized hydrogen atoms from the ground state into the final continuum states $m^{\pi_z} = 1^+$ (a) and $m^{\pi_z} = 0^-$ (b) at $B = 0.01$ a.u. (2350 T). Similar to Wang and Greene [17], the thicker (red) lines show our results after convolution with a Gaussian of width 0.0025 a.u. for $m^{\pi_z} = 1^+$ and 0.0009 a.u. for $m^{\pi_z} = 0^-$, respectively. The dashed vertical lines indicate the Landau thresholds in this regime.

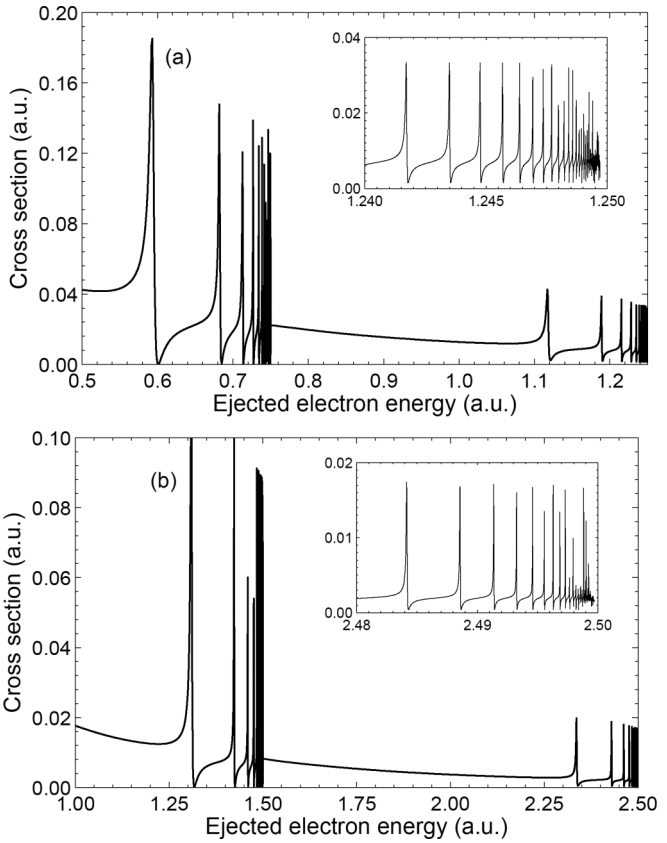

FIG. 6. Same as Fig. 5, except for photoionization from the ground state to the final continuum state $m^{\pi_z} = 0^-$ at $B = 0.5$ a.u. (117 500 T) (a) and $B = 1.0$ a.u. (235 000 T) (b). The insert in each panel displays the detailed resonance structure below the third Landau threshold.

Rydberg states and the Landau continuum states. For example, the first resonance above the first Landau threshold displays a pronounced asymmetric line shape, thus indicating a strong resonance-background interference. Similarly asymmetric line shapes are also seen above the second Landau threshold in this figure. The detailed resonance structure over a narrow ejected-electron energy region from 0.34 to 0.35 a.u., just below the third Landau threshold, is exhibited in the insert of the graph.

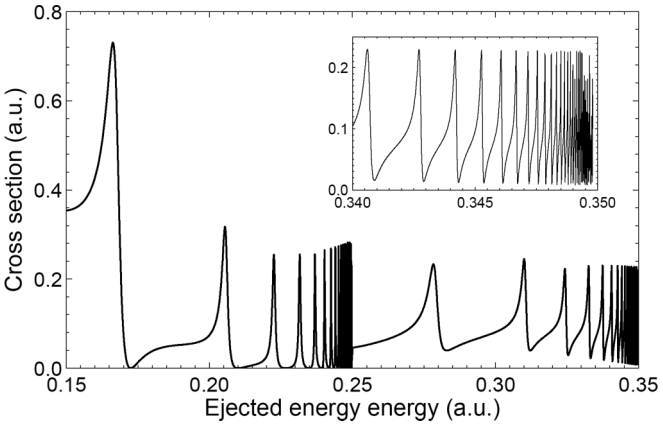

FIG. 5. Cross section for photoionization from the $2p_0$ excited state to the final $m^{\pi_z} = 1^-$ state for $B = 0.1$ a.u. (23 500 T). The insert displays the detailed resonance structure over a narrow ejected-electron energy region from 0.34 to 0.35 a.u., just below the third Landau threshold.

Figure 6 illustrates photoionization spectra from the ground state to the final continuum state with $m^{\pi_z} = 0^-$ at $B = 0.5$ a.u. (117 500 T) and $B = 1.0$ a.u. (235 000 T). The two spectra were calculated earlier with the complex-rotation method [18], but then only the first few dominant resonances were found to be stable against small variations in the numerical details. Contrary to the spectra from the complex-rotation method, for both $B = 0.5$ a.u. and $B = 1.0$ a.u., our coupled-channel formalism produces many resonances converging to the second and third Landau thresholds. The regularity of these resonance sequences is also visible in those two spectra.

IV. SUMMARY AND CONCLUSIONS

We have developed a theoretical method, based on the coupled-channel formalism, to study photoionization of H atoms in a strong magnetic field of strength typical for magnetic white dwarf stars. After expanding the total wave function in Landau states, the resulting coupled Schrödinger

equations are solved numerically using the renormalized Numerov method proposed by Johnson [25]. This algorithm propagates the ratio of the wave function at two adjacent points, rather than the wave function itself. Consequently, it effectively avoids overflow problems in the classically forbidden region. The present theoretical method was applied to calculations of continuous spectra due to photoionization from the ground state and excited states at selected magnetic fields.

Our calculations reproduced the benchmark spectra for photoionization from the ground state to the final continuum state with $m^{\pi_z} = 0^-$ at $B = 0.1$ a.u. (23 500 T). The spectra for a field strength of $B = 0.05$ a.u. (11 750 T) for the transition from the ground state to the final states with $m^{\pi_z} = 1^+$ and 0^- are also in excellent agreement with those calculated using the R-matrix method based on MQDT, as developed by Wang and Greene [17]. However, we found some differences in the photoionization spectrum at $B = 0.0085$ a.u. (2000 T) from the ground state to the final continuum state with $m^{\pi_z} = 1^+$, when calculated with our method or by other theories. Specifically, like Wang and Greene [17] and Meinhardt and co-workers [20], we disagree already in the qualitative energy dependence of the spectrum with the predictions of Alijah *et al.* [14]. Regarding the predictions of Wang and Greene [17], the qualitative agreement is satisfactory, although some quantitative differences were found at the lower field strengths of 2000 and 2350 T.

ACKNOWLEDGMENTS

L.B.Z. appreciates the hospitality and kindness of his colleagues at Drake University where this work was completed. We gratefully acknowledge financial support by the National Science Foundations of China, under Grant No. 11474079 (L.B.Z.), and the United States under Grants No. PHY-1430245 (K.B.) and No. PHY-1520970 (O.Z. and K.B.).

[1] R. H. Garstang, Rep. Prog. Phys. **40**, 105 (1977).
[2] H. Ruder, G. Wunner, H. Herold, and F. Geyer, *Atoms in Strong Magnetic Fields* (Springer-Verlag, Heidelberg, 1994).
[3] L. Ferrario, D. de Martino, and B. T. Gänsicke, Space Sci. Rev. **191**, 111 (2015).
[4] C. Schimeczek and G. Wunner, Astrophys. J., Suppl. Ser. **212**, 26 (2014).
[5] L. B. Zhao, B. C. Saha, and M. L. Du, Commun. Theor. Phys. **56**, 481 (2011).
[6] D. Baye, M. Hesse, and M. Vincke, J. Phys. B **41**, 185002 (2008).
[7] W. Rösner, G. Wunner, H. Herold, and H. Ruder, J. Phys. B **17**, 29 (1984).
[8] M. V. Ivanov and P. Schmelcher, Phys. Rev. A **61**, 022505 (2000).
[9] A. Thirumalai and J. S. Heyl, Phys. Rev. A **79**, 012514 (2009); **89**, 052522 (2014).
[10] A. Thirumalai, S. J. Desch, and P. Young, Phys. Rev. A **90**, 052501 (2014).
[11] C. Schimeczek and G. Wunner, Comput. Phys. Commun. **185**, 2655 (2014).
[12] W. Becken, P. Schmelcher, and F. K. Diakonos, J. Phys. B **32**, 1557 (1999).
[13] X. Wang, J. Zhao, and H. Qiao, Phys. Rev. A **80**, 053425 (2009).
[14] A. Alijah, J. Hinze, and J. T. Broad, J. Phys. B **23**, 45 (1990).
[15] B. R. Johnson, J. Comput. Phys. **13**, 445 (1973).
[16] D. Delande, A. Bommier, and J. C. Gay, Phys. Rev. Lett. **66**, 141 (1991).
[17] Q. Wang and C. H. Greene, Phys. Rev. A **44**, 7448 (1991).
[18] L. B. Zhao and P. C. Stancil, Phys. Rev. A **74**, 055401 (2006).
[19] L. B. Zhao and P. C. Stancil, Astrophys. J. **667**, 1119 (2007).
[20] G. Meinhardt, W. Schweizer, H. Herold, and G. Wunner, Eur. Phys. J. D **5**, 23 (1999).
[21] F. Mota-Furtado and P. F. O'Mahony, Phys. Rev. A **76**, 053405 (2007).
[22] L. D. Landau and E. M. Lifshitz, *Quantum Mechanics: Non-relativistic Theory* (Elsevier, Amsterdam, 1981).
[23] H. Friedrich and M. Chu, Phys. Rev. A **28**, 1423 (1983).
[24] M. J. Seaton, Rep. Prog. Phys. **46**, 167 (1983).
[25] B. R. Johnson, J. Chem. Phys. **67**, 4086 (1977); **69**, 4678 (1978).
[26] L. B. Zhao and P. C. Stancil, J. Phys. B **40**, 4347 (2007).